Heterolytic Scission of Hydrogen Within a Crystalline Frustrated Lewis Pair

Mark E. Bowden[a,*], Bojana Ginovska[b,*], Martin Owen Jones[c, d], Abhijeet J. Karkamkar[b], Anibal J. Ramirez-Cuesta[e], Luke L. Daemen[e], Gregory K. Schenter[b], Seth A. Miller[b], Timo Repo[f], Konstantin Chernichenko[f,1] Noemi Leick[g], Madison B. Martinez[g], and Tom Autrey[b]

a. *Environmental Molecular Sciences Laboratory, Pacific Northwest National Laboratory, PO Box 999 Richland, WA 99352, USA*

b. *Physical and Computational Sciences Directorate, Pacific Northwest National Laboratory, PO Box 999 Richland, WA 99352, USA*

c. *ISIS Neutron and Muon Spallation Facility, STFC, RAL, Didcot OX11 0QX, UK*

d. *St Andrews University, St Andrews, Fife KY16 9AJ, Scotland UK*

e. *Spallation Neutron Source, Oak Ridge National Laboratory, TN 37830, USA*

f. *Department of Chemistry, University of Helsinki, P.O. Box 55, 00014 Helsinki, Finland*

g. *National Renewable Energy Laboratory, 15013 Denver West Parkway, Golden, CO 80403, USA*

*mark.bowden@pnnl.gov, bojana.ginovska@pnnl.gov

Supporting Information

[1] Present address: *Janssen Pharmaceutica N.V., API Small Molecule Development, Turnhoutseweg 30, 2340 Beerse, Belgium*

Samples and handling

All manipulations were carried out under an inert (N_2) atmosphere using standard Schlenk or glovebox techniques unless otherwise stated. Samples of KCAT were synthesized according to published procedures.[1]

NMR Spectroscopy

NMR spectra were recorded in d_5-bromobenzene on a 500 MHz Varian INOVA spectrometer equipped with a boron-free 5-mm dual broadband gradient probe.

Powder Diffraction

Finely ground crystals of KCAT and KCATH2 were loaded under N_2 into thin wall 0.5 mm diameter capillaries (Charles Supper Company, MA) and sealed with wax. Powder diffraction patterns were recorded on a Rigaku Rapid-II microbeam diffractometer equipped with a Cr rotating anode x-ray source operated at 35 kV and 25 mA. The diffracted intensities were recorded on a 2D image plate and integrated to give 1D diffractograms.

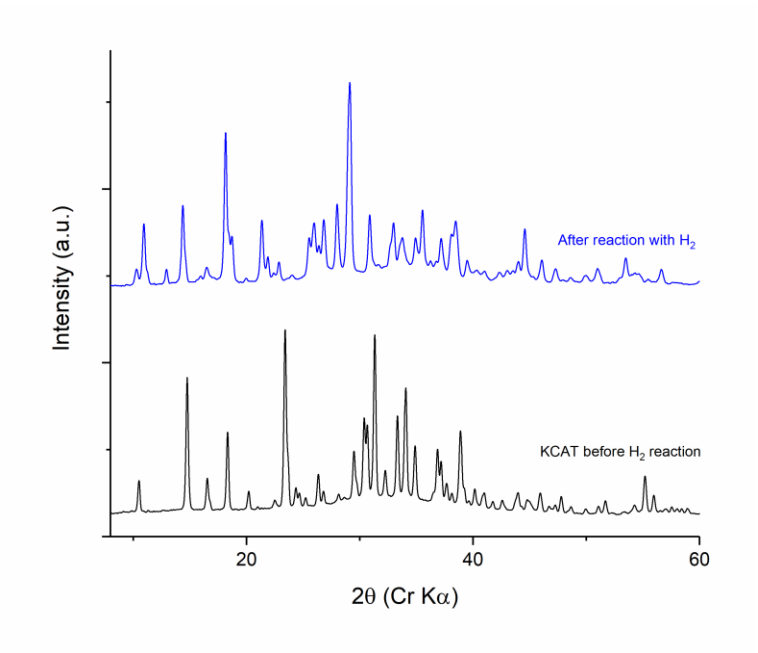

Figure S1. X-ray powder diffractograms of KCAT before (below) and after (above) reaction with H_2 gas at ambient conditions. Only traces of the starting FLP may be present in the hydrogenated product and both compounds appear fully crystalline. The broad background near 32° 2θ arises from the glass capillary used to contain the specimen.

Single Crystal Diffraction

A crystal of the transparent reaction product was mounted on a nylon loop. A Bruker Apex II diffractometer with Mo K_α radiation was used to record 2θ and ω scans at 100 K. Absorption corrections were applied using the multiscan method and the structure was solved using SHELXTL and refined with OLEX2. Hydrogen atoms bonded to carbon were restrained to be in their expected coordination (AFIX instruction) with riding displacement parameters. The positions of hydrogens attached to B and N were refined without restraint. Displacement parameters for H were isotropic and those for other atoms anisotropic. Details of the structure are given in **Table S1**.

Table S1. Crystallographic information obtained from solvent-free KCATH2

Crystal Data		
	Chemical formula	$C_{27}H_{24}BF_{10}N$
	M_r	563.31
	Crystal system, space group	Monoclinic, $P\,2_1/n$
	Temperature (K)	100
	a, b, c (Å), β (°)	11.9605(3), 11.8680(3), 17.9961(5), 104.257(1)
	V (Å^3)	2475.82(11)
	Z	4
	Crystal size (mm)	0.15 x 0.15 x 0.15
Data Collection		
	Radiation type	Mo K_α
	Absorption correction	Multi-scan (SADABS; Bruker, 2001)
	μ (mm^{-1})	0.140
	T_{min}, T_{max}	0.694, 0.746
	No. of measured, independent and observed [$I > 2\sigma(I)$] reflections	28190, 7163, 5909
	R_{int} 0.062	0.0274
Refinement		
	$R[F^2 > 2\sigma(F^2)]$, $R(F^2)$, S	0.0397, 0.0486, 1.013
	No. of reflections	7163
	No. of parameters	362
	$\Delta\rho_{max}$, $\Delta\rho_{min}$ (e Å^{-3})	0.419, -0.306

Computer programs: APEX2 and SAINT,[2] SHELXTL[3], OLEX2[4]

An overlay of the molecular geometry of this structure with the solvent-containing crystal is shown in **Figure S2**. One of the pentafluorophenyl rings attached to boron is in a slightly different orientation, but the more interesting difference is the orientation of the piperidine ring. In the material containing solvent, the phenyl ring linking B and N is approximately

axial to the piperidine ring. In the crystal synthesized here by gas-solid reaction, the phenyl ring lies approximately equatorial to piperidine, which is the same orientation as found in the original KCAT structure. Computation[5] for KCAT showed the equatorial configuration to be 10 kJ mol^{-1} lower in energy than the axial configuration, but the axial configuration places the piperidine ring further from C_6D_6 in the solvent-containing compound.

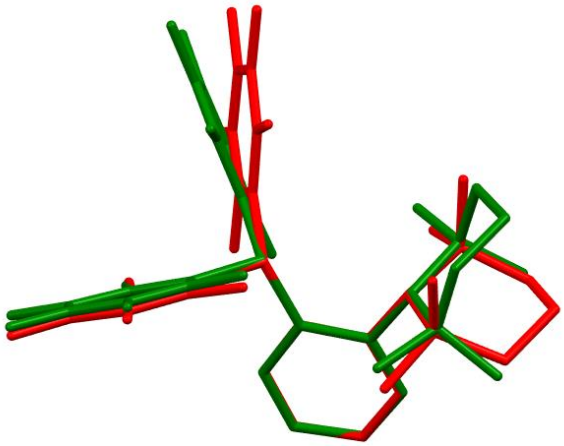

Figure S2. Overlay of structure of KCATH2 determined in this study (green) with that obtained from solvent crystallization[1] (red). The solvent molecules have been removed from the latter structure, and hydrogens removed for clarity.

Structures obtained for KCAT between 100 and 300 K were the same as previously published. The thermal density expansion calculated from the measured lattice parameters (**Figure S3**) (0.19 mg cm^{-3} K^{-1}) is the same as the average found in a survey of structures in the CSD.[6]

A comparison of selected bond lengths and angles around the B and N atoms in KCAT and KCATH2 is given in **Table S2**.

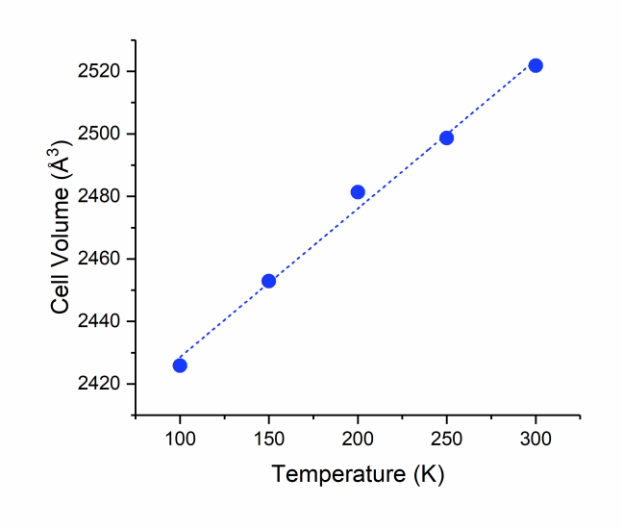

Figure S3. Cell volume of KCAT from single crystal measurements between 100 and 300 K.

Table S2. Comparison of selected interatomic distances (Å) and angles (°) in KCAT and KCATH2. Ph refers to the phenyl ring, PFPh1 and PFPh2 are the 2 pentafluorophenyl rings, and Pip1 and Pip2 are C atoms adjacent to N in the piperidene ring.

Distance/Angle	KCAT	KCATH2
B – C(Ph)	1.551(2)	1.640(1)
B – C(PFPh1)	1.584(2)	1.644(2)
B – C(PFPh2)	1.576(2)	1.641(2)
B – H	-	1.26(1)
C(Ph) – B – C(PFPh1)	121.3	114.3
C(Ph) – B – C(PFPh2)	120.2	112.6
C(PFPh1) – B – C(PFPh2)	117.3	107.4
N – C(Ph)	1.440(1)	1.487(1)
N – C(Pip1)	1.509(2)	1.562(1)
N – C(Pip2)	1.506(2)	1.558(2)
N – H	-	0.89(2)
C(Ph) – B – C(Pip1)	113.6	115.0
C(Ph) – B – C(Pip2)	116.4	116.4
C(Pip1) – B – C(Pip2)	118.0	117.6

Inelastic Neutron Scattering

Inelastic neutron scattering (INS) experiments were performed using the VISION spectrometer at the SNS neutron spallation facility, Tennessee, USA and the TOSCA spectrometer at the ISIS neutron spallation facility, UK.

VISION Spectrometer. 1.5 g (2.7 mmol) of finely ground KCAT were loaded into a proprietary gas exchange sample environment sample can under inert atmosphere. The can was sealed and connected to a gas control system, evacuated and transferred to the VISION spectrometer. Data were collected under vacuum at 10 K, 50 K, 100 K, 150 K and 200 K. The temperature was returned to 10 K and 3.6 mmol H_2 gas introduced before repeating data collection at the same temperatures. In order to prevent any gas-heating of sample and thereby potential hydrogen heterolysis by the FLP catalyst, the hydrogen gas was precooled prior to gas loading by passing it through a stainless coil immersed in liquid nitrogen. After the 200 K measurement, and with H_2 still present, a further measurement at 10 K was performed to limit line broadening by Debye-Waller effects. Finally, the specimen with the 3.6 mmol H_2 was heated to 298 K for 1 hr before a fourth 10 K measurement.

The data are shown in **Figure 4** and **Figure S4**. As no unambiguous signal for a bound hydrogen molecule could be observed in these data it is assumed that there is either no interaction between the hydrogen and the catalyst at these temperatures and pressures, or that the interaction is a purely surface event so that the concentration of bound hydrogen is too small to observe. Difference spectra (see example in **Figure 4**), removing the INS peaks from the total material, did not produce any observable signal for bound hydrogen thus eliminating the possibility that the signal had been masked

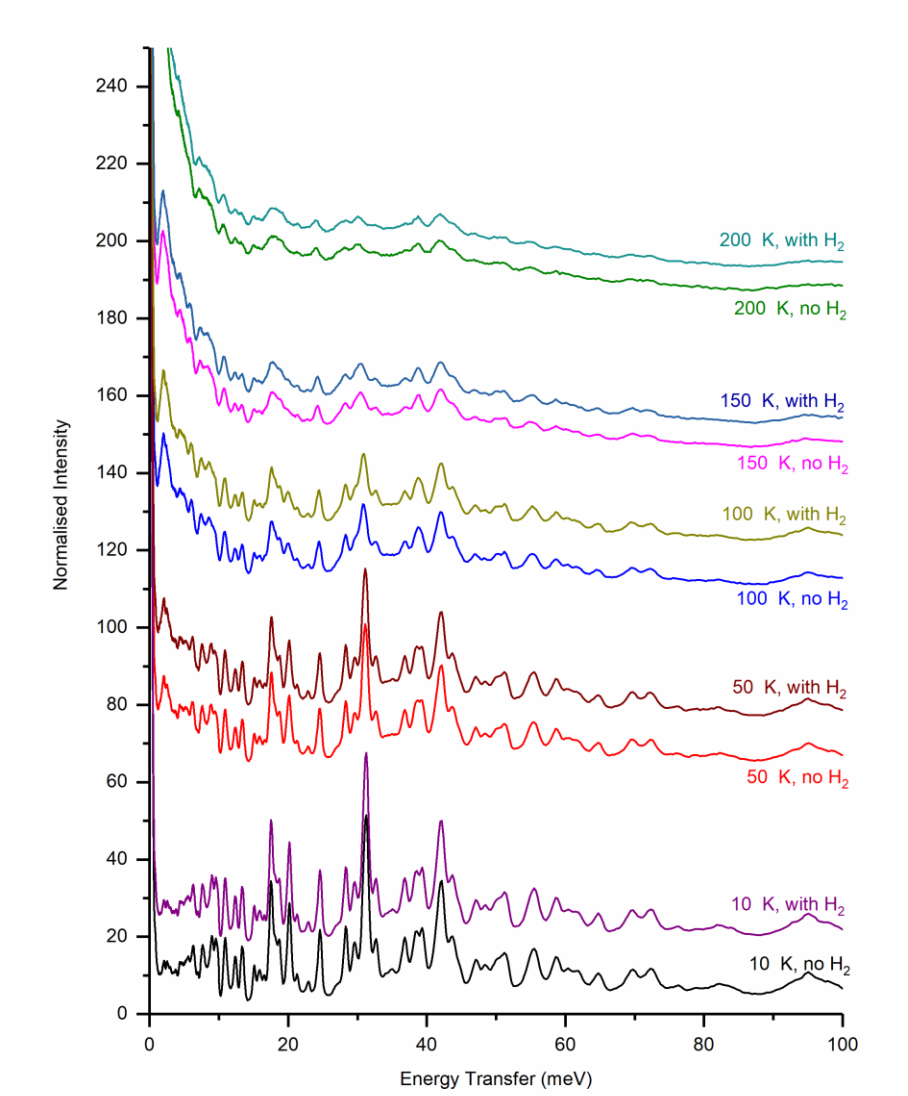

Figure S4. INS spectra recorded at VISION with and without H_2 at 10 – 200 K, offset for clarity.

TOSCA Spectrometer. 5 g of finely ground KCAT were loaded under inert atmosphere into an evacuable, cylindrical sample environment and sealed. The sample environment was then connected to a gas handling system and evacuated before being loaded into the TOSCA spectrometer. Data were collected under vacuum, 2 bar and 50 bar of hydrogen at 40 K. Again, in order to prevent any gas-heating of sample and potential hydrogen heterolysis by the FLP, the hydrogen gas was precooled prior to gas loading using a stainless coil immersed in liquid nitrogen.

Typical data sets at 40 K for KCAT (a) in vacuum and (b) under 50 bar H_2 are shown in **Figure S5**. Difference spectra (bare Material –Material + H_2) are also shown in **Figure S5**. Again, no unambiguous signal for a bound hydrogen molecule could be observed and therefore it is

assumed that there is either no interaction between the hydrogen and material at this temperatures and pressures, or that the concentration of bound hydrogen is too small to observe.

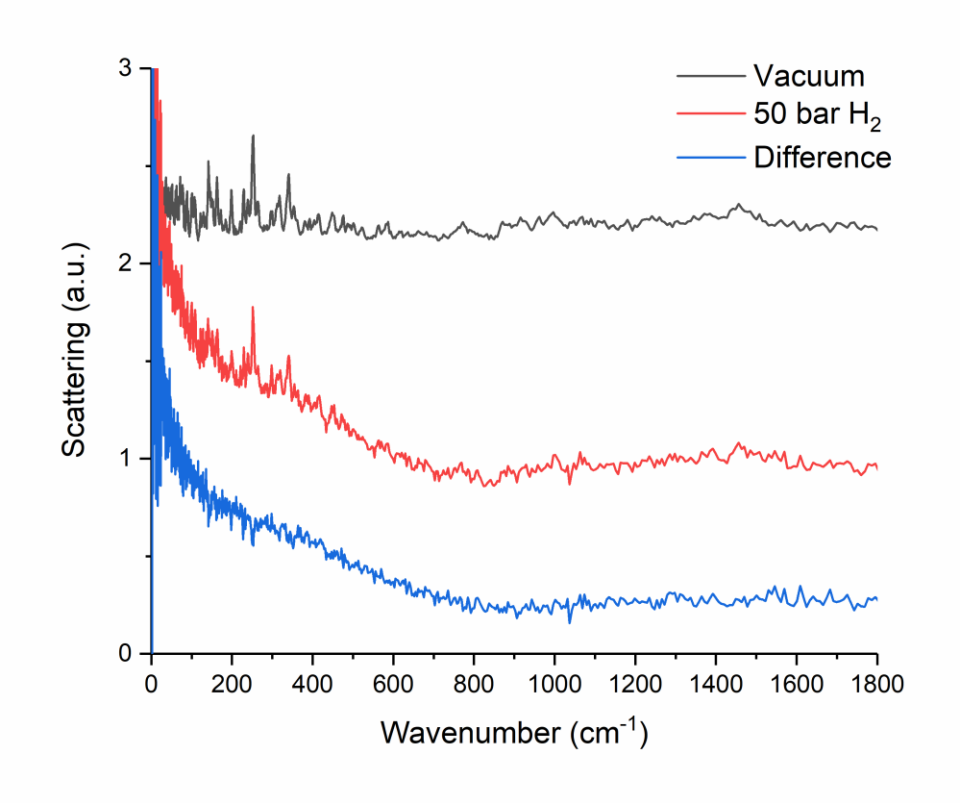

Figure S5. INS spectra recorded at TOSCA of KCat at 40K in vacuum and with 50 bar H_2 pressure. The difference between these is also shown, and the spectra are offset for clarity.

After data collection at 40K, the sample of KCAT was allowed to warm to room temperature under hydrogen atmosphere to form the corresponding ion pair, evacuated, cooled to 40K and data again collected. The data set for reacted KCAT, with the corresponding difference spectra (bare Catalyst– reacted catalyst) are shown in **Figure S6**. Here, a number of new peaks corresponding to the newly formed B-H and N-H bonds can be observed alongside a number of other modifications in the INS spectrum which result from the reorientation of the molecule on hydrogenation.

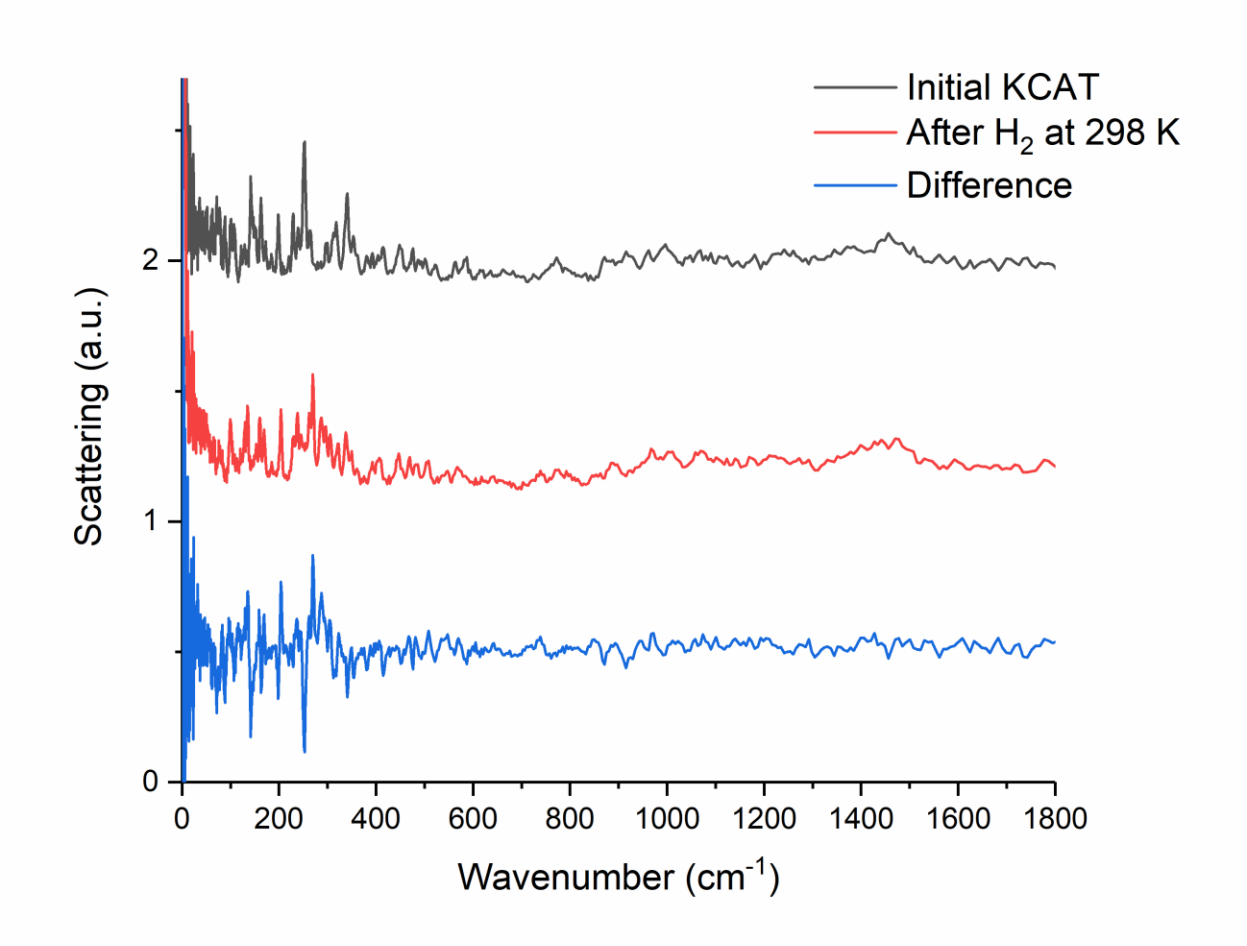

Figure S6. TOSCA INS Spectra of KCAT and KCATH2 at 40K with the corresponding difference.

Temperature Programmed Desorption

1 mg of KCAT was loaded into an envelope of platinum foil to ensure homogeneous heating over the entire sample and was subsequently placed in a quartz tube that was mounted to a custom-built temperature programmed desorption (TPD) system. A detailed description and characterization of the system can be found elsewhere.[7]

The specimen was first slowly heated to 350 K to desorb impurities, such as water. Then, it was exposed to 1 atm of H_2 gas for 5 and 30 minutes at 300 K and cooled rapidly to 77 K under H_2 atmosphere before pumped to *ca*. 1 x 10^{-8} Torr. The temperature was then raised to 330 K at 5 K/min, using a DigiSense temperature controller, and any gas liberated was measured using a Stanford Research Systems RGA 100 residual gas analyzer, operating at 70 eV ionization energy. The traces corresponding to H_2 gas are shown in **Figure S7**. There was no H_2 evolution from the specimen detected; the gradual decline after the 5-minute exposure amounts to a slow evacuation of background signal.

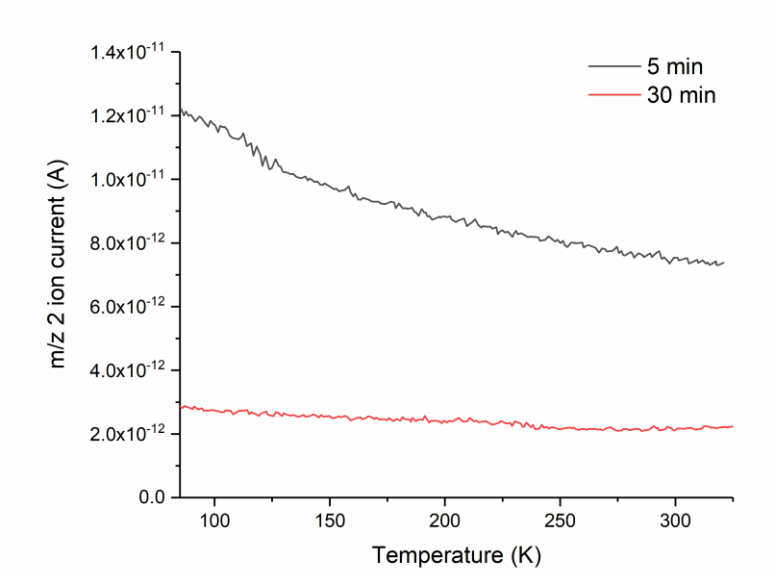

Figure S7. H_2 (m/z 2) signals from TPD after exposing KCAT crystals to 1 atmosphere H_2 at 300 K for 5 and 30 minutes.

Computational modeling

DFT calculations and MD simulations were carried out using the CP2K electronic structure package.[8] A DZVP basis set was used with the PBE[9] and Grimme D2[10] dispersion correction. Goedeker-Hutter pseudopotentials[11] consistent with the PBE functional were employed. The calculations were initiated from crystal structure geometries for KCAT and KCATH2 using the lattice parameters determined experimentally and were treated periodically, with the $P2_1/c$ symmetry removed to leave 4 independent KCAT molecules in the monoclinic unit cell. The electronic energies were calculated by adding 4 H_2 molecules to the KCAT crystal structure and were also optimized after each added H_2 molecule using the Conjugate Gradient method. Minima on the potential energy surface were confirmed by the absence of imaginary frequencies in the vibrational analysis in harmonic oscillator framework. Free energy calculations were obtained from the vibrational analysis using the harmonic expression for the Helmholtz free energy:

$$A = E_0 + \sum_i^N \frac{\omega_i \hbar}{2} + k_B T log(1 - e^{\frac{-\omega_i \hbar}{k_B T}})$$

The harmonic Hamiltonian was also used to generate INS spectra using the aCLIMAX code.[12] The calculated spectra are shown in **Figure S8** which indicates that the presence of H_2 in the KCAT lattice should show up in the difference spectra. The positions of each of the four H_2 molecules are shown in **Figure S9**.

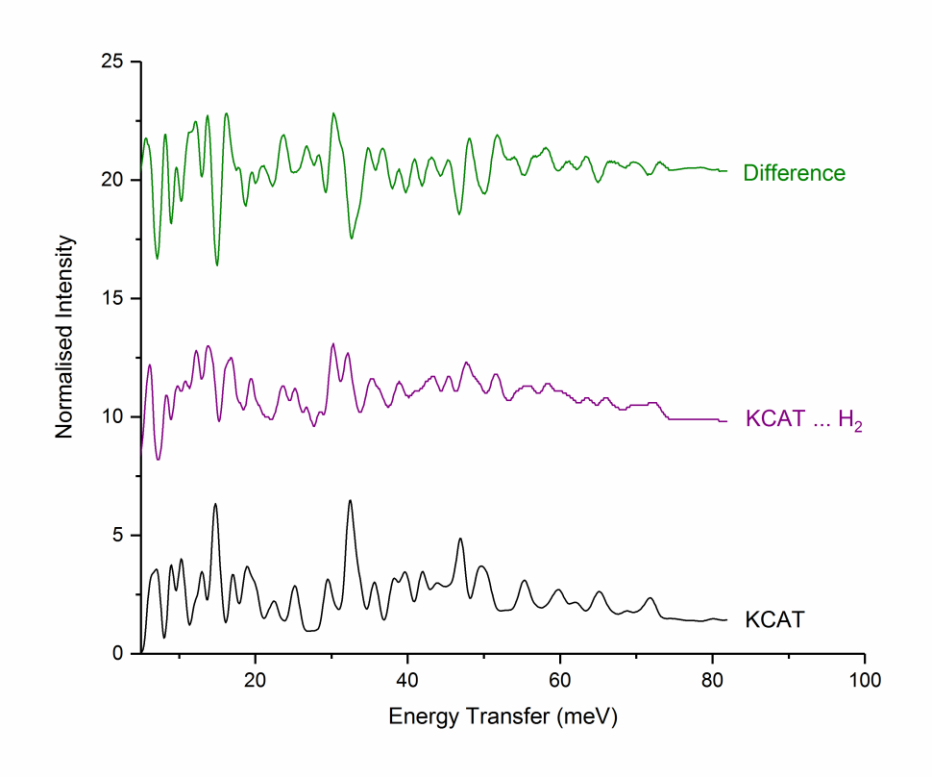

Figure S8. Calculated INS spectra for KCAT with and without H_2 in the lattice.

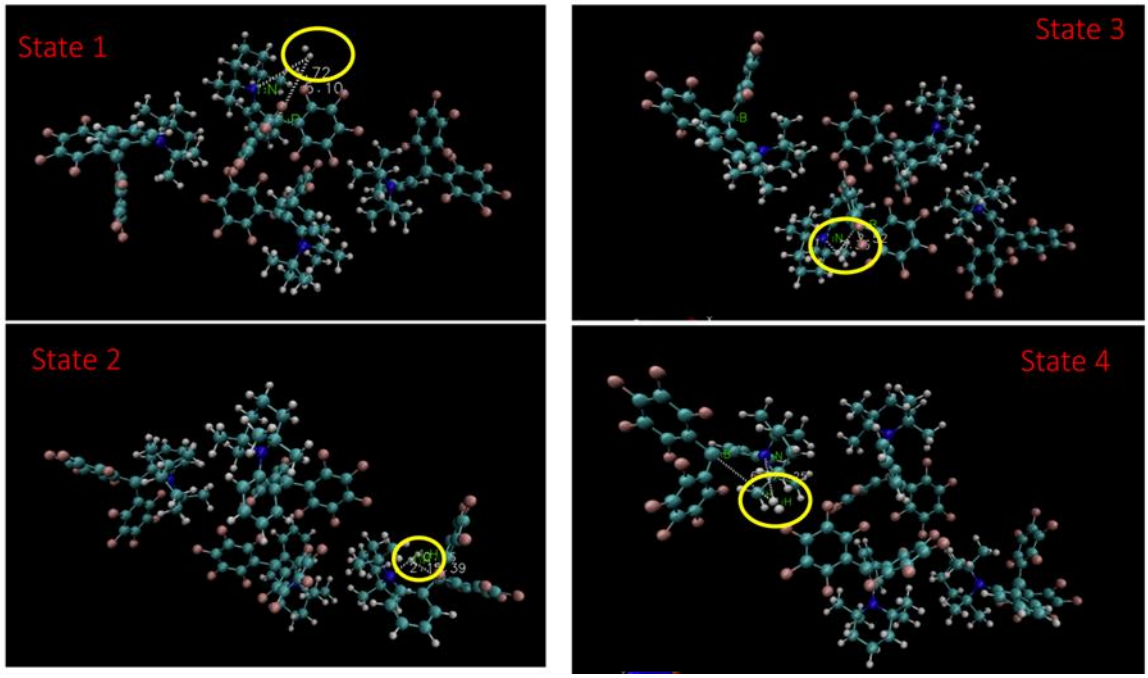

Figure S9. Locations of the four different H_2 molecules optimized in a single unit cell of KCAT. The energies and interatomic distances associated with these sites are presented in Table 1.

From the harmonic analysis, it is possible to evaluate the classical Debye-Waller factor and obtain the thermal ellipsoids corresponding to the delocalization of the H_2. Large delocalization is indicative of large flexibility of the motions. These large amplitude yet bound motions are consistent with the extra features that appear in the calculated INS spectra. Examples of these are displayed in **Figure S10**.

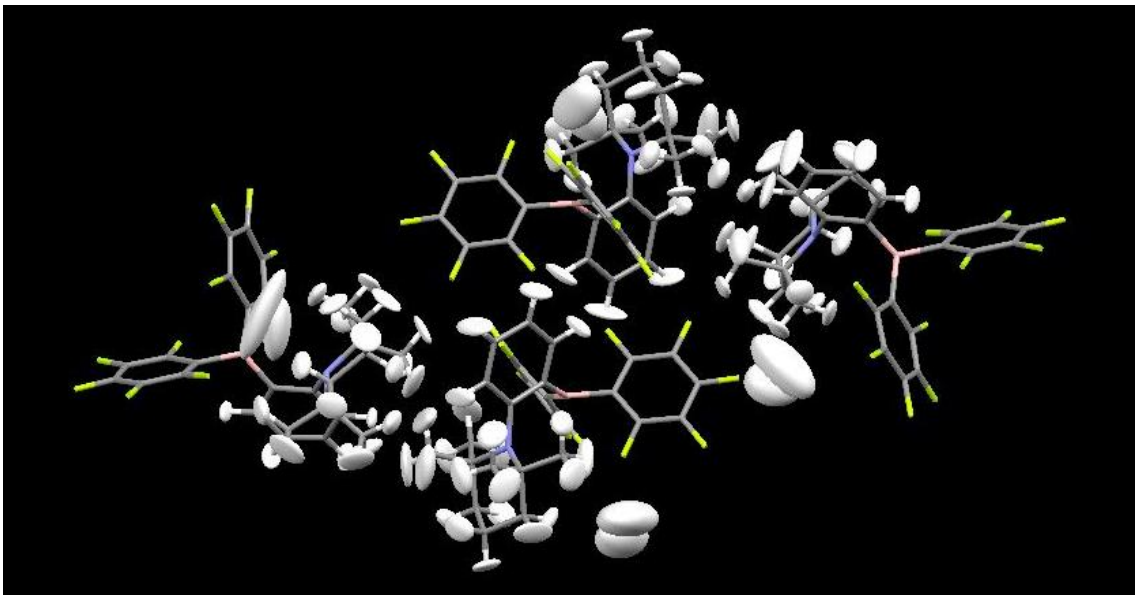

Figure S10. Ellipsoids for hydrogen atoms in KCAT with additional molecules of H_2

Ab Initio Molecular Dynamics (MD) simulation studies were also carried out at the same level of theory as the harmonic DFT calculations, within the NVE ensemble, at temperatures of 160, 250 and 310 K. A time step of 0.25 ps was used, and trajectories of 12 ps were generated after a 5 ps equilibration. A velocity autocorrelation was used to follow the motion of the H_2 molecules confined within the KCAT structure. A plot of the trajectories taken by the four H_2 molecules is shown in **Figure S11**, and the distances from their starting positions shown in **Figure S12**.

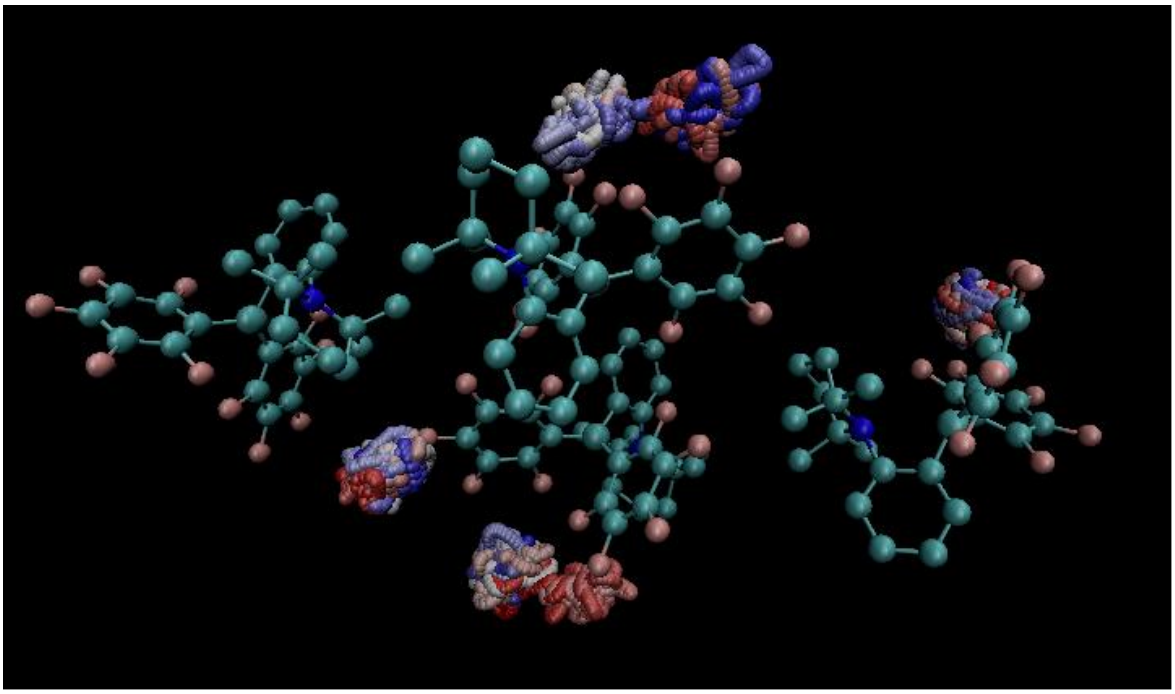

Figure S11. Positions of H_2 (small spheres) within KCAT superimposed for each time step during the MD simulation. The starting positions are colored blue and the final positions red. The larger spheres show the positions of KCAT atoms with hydrogens omitted for clarity.

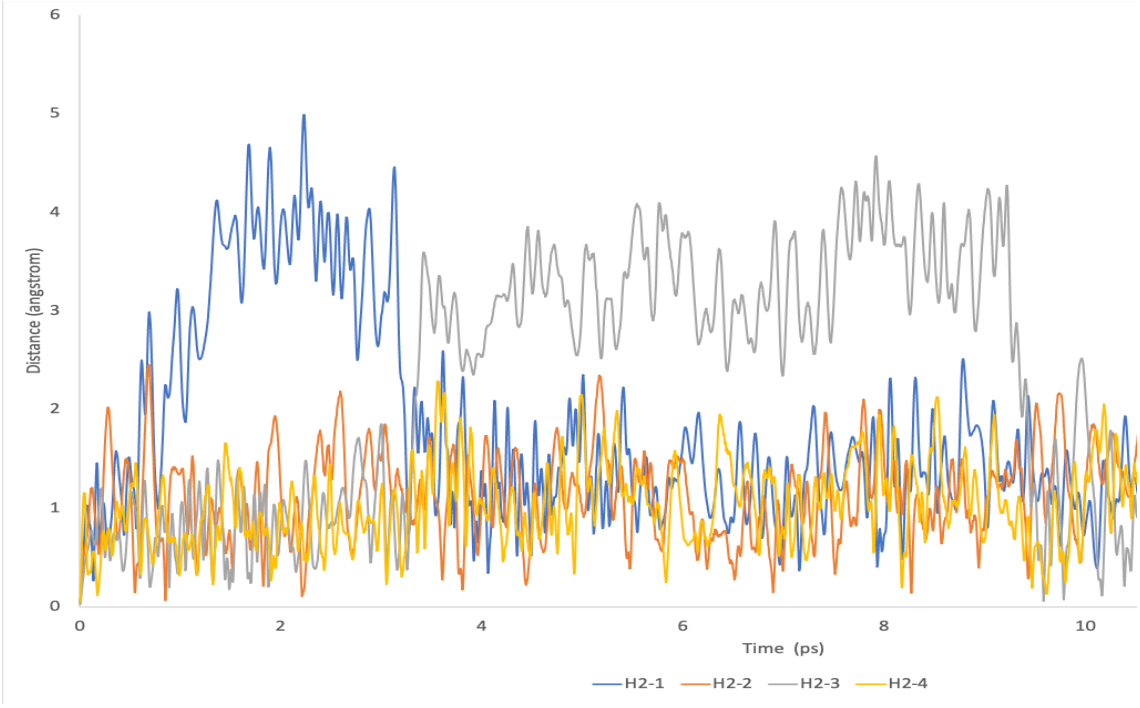

Figure S12. Distances for each of the H_2 molecules within KCAT during the MD simulation measured from their equilibrated starting positions.

The MD studies take anharmonicity into account in the motions that are not included with the harmonic treatment in the vibrational analysis of the stable structures. From a Fourier transformation of the *ab initio* velocity autocorrelation (VAC) function of the H_2 motion, the anharmonic spectra can be obtained and directly compared with the INS spectra. The VAC function is given as $C_{vv}(t)$:

$$C_{vv}(t) = \frac{1}{N}\sum_{j=1}^{N}\langle v_j(t) \cdot v_j(0)\rangle$$

The spectrum is obtained via:

$$I(\omega) = \int_{-\infty}^{+\infty} exp(i\omega t)\, C_{vv}(t)dt$$

In these equations, N is the number of hydrogen atoms and $v_j(t)$ is the velocity of hydrogen atom j at time t. Details of this approach can be found in our previous work.[13]

In each unit cell there are 4 H_2 molecules, and in **Figure S13** we report the spectrum for each separately. These spectra show a characteristic feature of a constrained H_2 motion ~200 cm-1 (~25 meV) that was observed in the calculated INS spectra from the harmonic treatment, showing consistent observation between the two approaches.

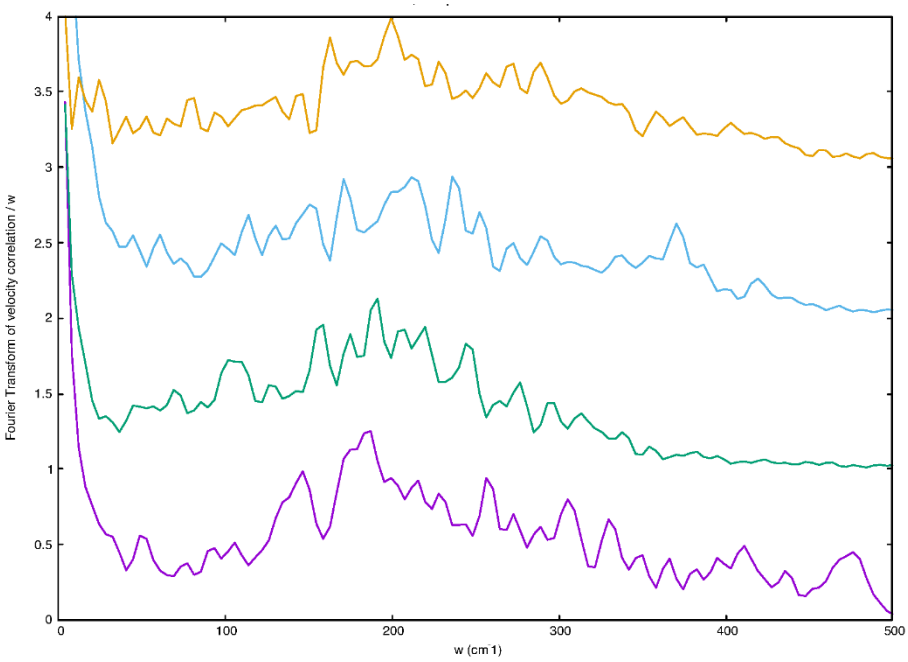

Figure S13. Calculated INS spectra for each of the H_2 molecules within KCAT from the MD simulation, offset for clarity.

References

1. Chernichenko, K.; Nieger, M.; Leskela, M.; Repo, T., Hydrogen activation by 2-boryl-N,N-dialkylanilines: a revision of Piers' ansa-aminoborane. *Dalton T* **2012,** *41* (30), 9029-9032.
2. Bruker Bruker ASX, Madison, WI, 2012.
3. Sheldrick, G., Crystal structure refinement with SHELXL. *Acta Crystallographica Section C* **2015,** *71* (1), 3-8.
4. Dolomanov, O. V.; Bourhis, L. J.; Gildea, R. J.; Howard, J. A. K.; Puschmann, H., OLEX2: a complete structure solution, refinement and analysis program. *J Appl Crystallogr* **2009,** *42*, 339-341.
5. Chernichenko, K.; Kotai, B.; Nieger, M.; Heikkinen, S.; Papai, I.; Repo, T., Replacing C6F5 groups with Cl and H atoms in frustrated Lewis pairs: H-2 additions and catalytic hydrogenations. *Dalton T* **2017,** *46* (7), 2263-2269.
6. Sun, C. C., Thermal expansion of organic crystals and precision of calculated crystal density: a survey of Cambridge Crystal Database. *J Pharm Sci* **2007,** *96* (5), 1043-52.
7. Hurst, K. E.; Heben, M. J.; Blackburn, J. L.; Gennett, T.; Dillon, A. C.; Parilla, P. A., A dynamic calibration technique for temperature programmed desorption spectroscopy. *Rev Sci Instrum* **2013,** *84* (2), 025103.
8. VandeVondele, J.; Krack, M.; Mohamed, F.; Parrinello, M.; Chassaing, T.; Hutter, J., Quickstep: Fast and accurate density functional calculations using a mixed Gaussian and plane waves approach. *Computer Physics Communications* **2005,** *167* (2), 103-128.
9. Perdew, J. P.; Burke, K.; Ernzerhof, M., Generalized Gradient Approximation Made Simple. *Phys Rev Lett* **1996,** *77* (18), 3865-3868.
10. Grimme, S., Semiempirical GGA-type density functional constructed with a long-range dispersion correction. *J Comput Chem* **2006,** *27* (15), 1787-99.
11. Goedecker, S.; Teter, M.; Hutter, J., Separable dual-space Gaussian pseudopotentials. *Phys Rev B Condens Matter* **1996,** *54* (3), 1703-1710.
12. Ramirez-Cuesta, A. J., aCLIMAX 4.0.1, The new version of the software for analyzing and interpreting INS spectra. *Computer Physics Communications* **2004,** *157* (3), 226-238.
13. Kathmann, S. M.; Mundy, C. J.; Schenter, G. K.; Autrey, T.; Aeberhard, P. C.; David, B.; Jones, M. O.; Ramirez-Cuesta, T., Understanding Vibrational Anharmonicity and Phonon Dispersion in Solid Ammonia Borane. *The Journal of Physical Chemistry C* **2012,** *116* (9), 5926-5931.